DOI 10.5012/bkcs.2010.31.6.1665

Determination of Strongly Interacting Spin Exchange Path and Spin Lattice Model of $(VO)_2(H_2O)\{O_3P\text{-}(CH_2)_3\text{-}PO_3\}\cdot 2H_2O$ on the Basis of Spin Dimer Analysis

Dae Hyun Kim and Hyun-Joo Koo*

Department of Chemistry and Research institute of Basic Sciences, Kyung Hee University, Seoul 130-701, Korea
**E-mail: hjkoo@khu.ac.kr*
Received January 26, 2010, Accepted April 8, 2010

The spin exchange interactions of $(VO)_2(H_2O)\{O_3P\text{-}(CH_2)_3\text{-}PO_3\}\cdot 2H_2O$ were examined by spin dimer analysis based on extended Hückel tight binding method. The strongest spin exchange interaction occurs through the super-super-exchange path J_2 and the second strongest spin exchange interaction occurs through the superexchange interaction path J_1. There are two strongly interacting spin exchange paths in $(VO)_2(H_2O)\{O_3P\text{-}(CH_2)_3\text{-}PO_3\}\cdot 2H_2O$. Therefore, magnetic susceptibility curve of $(VO)_2(H_2O)\{O_3P\text{-}(CH_2)_3\text{-}PO_3\}\cdot 2H_2O$ can be well reproduced by an alternating one-dimensional antiferromagnetic chain model rather than an isolated spin dimer model.

Key Words: Spin dimer analysis, Magnetic orbital, Spin exchange interactions, Electronic structure calculations

Introduction

The spin-lattice of a magnetic solid is determined by the repeat pattern of its strongly interacting spin exchange interactions.[1-6] For instance, a magnetic solid described by an alternating antiferromagnetic (AFM) chain model has a chain of alternating exchange interactions J and J'. Spin exchange interactions between adjacent ions in a given magnetic solid take place through either superexchange (SE) paths or super-superexchange (SSE) paths.[2,7] SSE interactions can be much stronger than SE interactions but have frequently ignored without justifiable reasons. To find a spin-lattice model relevant for a magnetic oxide, the relative strengths of both SE and SSE interactions should be evaluated on the basis of proper electronic structure considerations. The spin dimer analysis based on tight binding electronic structure calculations has been indispensible for a variety of magnetic oxides, because it reproduces the relative strengths of spin exchange interactions determined from first principles electronic structure calculations as well as it can be applied for the systems which are hard to be treated by first principles electronic structure calculations due to the numerous atoms in a unit cell.[1-7]

In the analysis of the magnetic susceptibility data with a spin Hamiltonian, the associated exchange parameters become numerical fitting parameters that reproduce the experimental data. This fitting analysis may not provide a unique solution, and there are cases when magnetic susceptibility data can be fitted equally well with more than one spin-lattice model. For example, vanadyl pyrophosphate $(VO)_2P_2O_7$ has a spin gap and its magnetic susceptibility can be described by alternating AFM chain model[8] and two-leg spin ladder model.[9,10] It is an important issue to determine which model is correct in such a case. An alternating AFM chain was proven to be correct for $(VO)_2P_2O_7$ by neutron scattering experiments[11,12] with oriented crystal samples and also by spin dimer analysis based on tight binding electronic structure calculations.[1,7b]

Vanado-alkyldiphosphonate $(VO)_2(H_2O)\{O_3P\text{-}(CH_2)_3\text{-}PO_3\}\cdot 2H_2O$, which is a pillared compound built up by alternating of inorganic slabs and the propyl chains along the [100] direction, is synthesized hydrothermally and its magnetic properties are examined by performing magnetic susceptibility measurement.[13] Observed magnetic susceptibility curve shows a broad maximum around $T_{max} \approx 60$ K and decreases rapidly below T_{max}, which are characteristic behavior of a spin-gapped low-dimensional antiferromagnet.[13] (Here T_{max} is the temperature at which magnetic susceptibility χ reaches its maximum χ_{max}) The magnetic susceptibility curve was fitted by using an isolated spin dimer model of Bleaney-Bowers[14] and by using Ising spin dimer model.[13] The fitting result shows that the magnetic susceptibility data were well reproduced by using the Bleaney-Bowers equation with $J/k_B = -42.4$ K and $g = 1.984$ rather than using the Ising model. However, Riou *et al*.[13] pointed out that the theoretical magnetic susceptibility curve of $(VO)_2(H_2O)\{O_3P\text{-}(CH_2)_3\text{-}PO_3\}\cdot 2H_2O$ is rather strongly deviated from the theoretical plot when they compare with the result for $VO(HPO_4)\cdot 0.5H_2O$,[15] which shows highly precise fit to the Bleaney-Bowers equation. They conclude that the poorer fit of the $(VO)_2(H_2O)\{O_3P\text{-}(CH_2)_3\text{-}PO_3\}\cdot 2H_2O$ is due to a long-range weak magnetic interactions between the spin dimers, which is not taken into account in Bleaney-Bowers equation. In the present work, to determine a precise spin-lattice model for $(VO)_2(H_2O)\{O_3P\text{-}(CH_2)_3\text{-}PO_3\}\cdot 2H_2O$, we evaluate the spin exchange interactions of $(VO)_2(H_2O)\{O_3P\text{-}(CH_2)_3\text{-}PO_3\}\cdot 2H_2O$ by performing a spin dimer analysis based on extended Hückel tight binding (EHTB) calculations.

Structure and Spin Dimer Analysis

The crystal structure of $(VO)_2(H_2O)\{O_3P\text{-}(CH_2)_3\text{-}PO_3\}\cdot 2H_2O$ is made up of isolated $V_2O_8(H_2O)$ and propylenediphosphonate units (Figure 1a). Each $V_2O_8(H_2O)$ unit is obtained from two $VO_5(H_2O)$ octahedral units by sharing their one face. In the $VO_5(H_2O)$ octahedron, the V-O bond distances are 1.594, 2.086 (×2), 1.927 (×2) and 2.365 Å, respectively. The isolated $V_2O_8(H_2O)$ dimer units are linked by $P_2O_6C_3H_6$ unit so it forms a chain of $V_2O_8(H_2O)$ dimer along the c-axis (Figure 1b). Each $V_2O_8(H_2O)$ dimer chains are connected by propylenediphos-

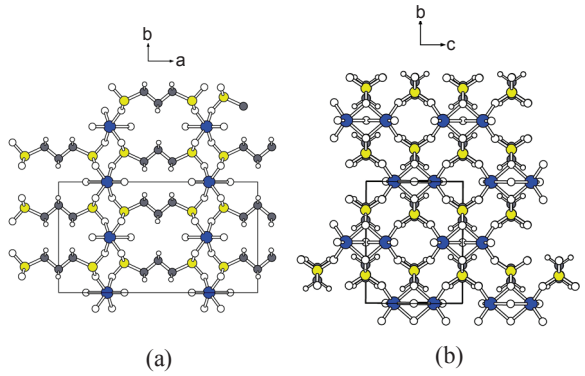

Figure 1. Projection view of crystal structure of $(VO)_2(H_2O)\{O_3P\text{-}(CH_2)_3\text{-}PO_3\}\cdot 2H_2O$ along the (a) c-direction and (b) a-direction. The blue, yellow, gray, large white and small white circles represent V, P, C, O and H atoms, respectively.

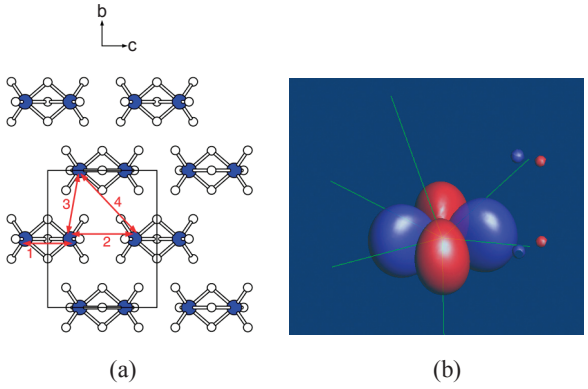

Figure 2. (a) Schematic representation of the spin exchange paths for $(VO)_2(H_2O)\{O_3P\text{-}(CH_2)_3\text{-}PO_3\}\cdot 2H_2O$. The numbers 1, 2, 3 and 4 indicate the spin exchange paths J_1, J_2, J_3 and J_4, respectively. For simplicity, C, P and H atoms are removed. (b) Schematic representation of the magnetic orbital of VO_6 octahedral unit.

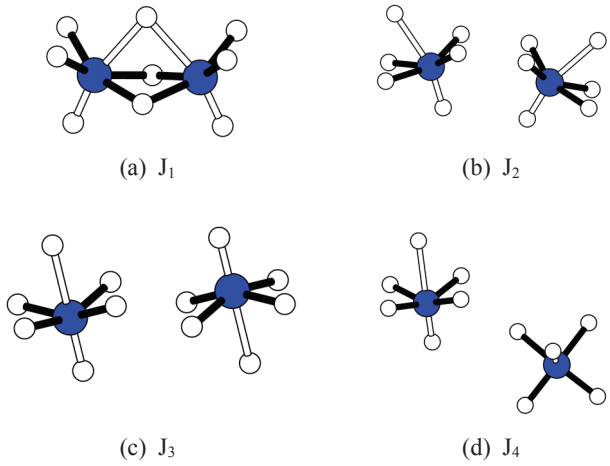

Figure 3. The spin dimers associated with the spin exchange paths (a) J_1, (b) J_2, (c) J_3 and (d) J_4, respectively. The black cylinders represent the V-O bonds in basal plane.

phonate groups and hence it forms two dimensional network of $V_2O_8(H_2O)$ dimer in bc-plane (Figure 1b). In the $V_2O_8(H_2O)$ dimer chain, the axial oxygen atoms forming the shortest V-O bond have the *cis* arrangement, while the axial oxygen atoms between the adjacent $V_2O_8(H_2O)$ dimer chains have the *trans* arrangement. Along each $V_2O_8(H_2O)$ dimer chain, the SE interaction within $V_2O_8(H_2O)$ dimer and the SSE interaction between adjacent $V_2O_8(H_2O)$ dimers occur and they alternate. Additional SSE interactions occur between the $V_2O_8(H_2O)$ dimer chains. Therefore, there are four spin exchange interaction paths J_1, J_2, J_3, and J_4 in $(VO)_2(H_2O)\{O_3P\text{-}(CH_2)_3\text{-}PO_3\}\cdot 2H_2O$. The spin exchange paths J_1, J_2, J_3, and J_4 are shown in Figure 2(a) and the magnetic orbital of VO_6 octahedral spin monomer unit is shown in Figure 2(b).

The strength of a spin exchange interaction between two spin sites is described by a spin exchange parameter $J = J_F + J_{AF}$, where J_F is the ferromagnetic (FM) term ($J_F > 0$) and J_{AF} is the AFM term ($J_{AF} < 0$). In most cases, J_F is very small so that the trends in the J values are well approximated by those in the corresponding J_{AF} values. For a spin dimer in which each spin site contains one unpaired spin, the J_{AF} term is approximated by[2,16]

$$J_{AF} \approx \frac{(\Delta e)^2}{U_{eff}} \quad (1)$$

where U_{eff} is the effective on-site repulsion, which is essentially a constant for a given compound. If the two spin sites are equivalent, (Δe) is the energy difference between the two magnetic orbitals (i.e., singly occupied molecular orbitals of the spin monomers) representing the spin dimer. For a variety of magnetic solids of transition metal ions, it has been found that their magnetic properties are well described by the $(\Delta e)^2$ values obtained from EHTB calculations,[17,18] when both the d orbitals of the transition metal ions and the s/p orbitals of its surrounding ligands are represented by double-ζ Slater-type orbitals (DZ-STO).[1-7] The radial part of a DZ-STO is expressed as

$$r^{n-1}\left[c_1 \exp(-\zeta_1 r) + c_2 \exp(-\zeta_2 r)\right]$$

where n is the principal quantum number and the exponents ζ_1 and ζ_2 describe contracted and diffuse STOs, respectively (i.e., $\zeta_1 > \zeta_2$). The diffuse STO provides an orbital tail that enhances overlap between ligands of the SSE paths. The (Δe) values are affected most sensitively by the exponent ζ_2 of the diffuse O 2p orbital. The ζ_2 values taken from results of electronic structure calculations for neutral atoms may not be diffuse enough to describe O^{2-} ions.[19] To make the O 2p orbital more diffuse, the ζ_2 value should be reduced. To assess how the diffuseness the O 2p orbital affects the relative strengths of the super-super-exchange interactions between adjacent spin dimers, we replace ζ_2 with (1-x) ζ_2 and calculate the $(\Delta e)^2$ values for three values of x, i.e., 0.00, 0.05, 0.10.

Spin Exchange Interactions of the $(VO)_2(H_2O)\{O_3P\text{-}(CH_2)_3\text{-}PO_3\}\cdot 2H_2O$

The spin dimers associated with the spin exchange paths J_1, J_2, J_3 and J_4 are shown in Figure 3 and the geometrical parameters for the spin dimers are summarized in Table 1. The V

Table 1. Geometrical parameters associated with the spin exchange paths of $(VO)_2(H_2O)\{O_3P\text{-}(CH_2)_3\text{-}PO_3\}\cdot 2H_2O$.

(a) SE

Path	V···V	V—O	∠V—O—V
J_1	3.089	2.086, 2.086	95.5
		2.086, 2.086	95.5
		2.365, 2.365	81.5

(b) SSE

Path	V···V	O···O	V—O	∠V—O···O
J_2	4.368	2.507	1.927, 1.927	118.9, 118.9
		2.507	1.927, 1.927	118.9, 118.9
J_3	4.737	2.474	2.086, 1.927	101.7, 130.4
		2.474	1.927, 2.086	130.4, 101.7
J_4	5.995	2.474	2.086, 1.927	162.3, 130.4

The bond distances are in unit of Ångström and the bond angles are in units of degrees.

Table 2. Relative values of $(\Delta e)^2$ of the spin exchange paths in $(VO)_2(H_2O)\{O_3P\text{-}(CH_2)_3\text{-}PO_3\}\cdot 2H_2O$

Path	x = 0.00	x = 0.05	x = 0.10
J_1	0.81	0.45	0.19
J_2	1.00	1.00	1.00
J_3	0.00	0.00	0.00
J_4	0.00	0.00	0.00

Table 3. The Slater-type atomic orbital parameters used for extended Hückel tight binding calculations

Atom	χ_i	H_{ii}(eV)	ζ_1	C_1	ζ_2'	C_2
V	4s	−8.81	1.697	1.0		
V	4p	−5.52	1.260	1.0		
V	3d	−11.0	5.052	0.3738	2.173	0.7456
O	2s	−32.3	2.88	0.7076	1.675	0.3745
O	2p	−14.8	3.694	0.3322	1.659	0.7448
P	3s	−18.6	2.367	0.5846	1.499	0.5288
P	3p	−14.0	2.065	0.4908	1.227	0.5940
C	2s	−21.4	1.831	0.7931	1.153	0.2739
C	2p	−11.4	2.730	0.2595	1.257	0.8062
H	1s	−13.6	1.300	1.0		

H_{ii}'s are the diagonal matrix elements $\langle \chi_i | H^{eff} | \chi_i \rangle$, where H^{eff} is the effective Hamiltonian. In our calculations of the off-diagonal matrix elements $H_{ij} = \langle \chi_i | H^{eff} | \chi_j \rangle$, the weighted formula was used. See Ammeter, J.; Bürgi, H.-B.; Thibeault, J. C.; Hoffmann, R. *J. Am. Chem. Soc.* **1978**, *100*, 3686.

atoms in spin dimer units move toward the axial oxygen atom so the basal planes of the SSE path J_3 and J_4 are not coplanar unlike the SSE path J_2. The effective overlap between O···O

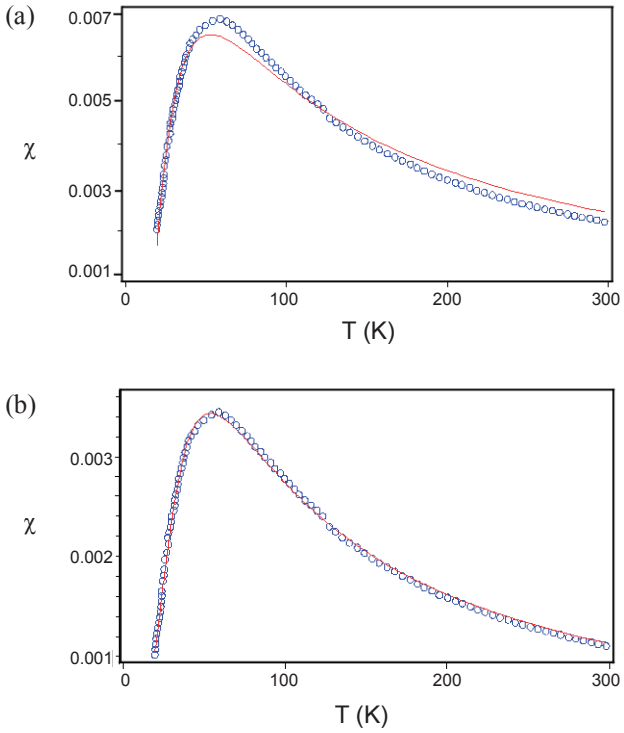

Figure 4. Numerically analyzed magnetic susceptibility of $(VO)_2(H_2O)\{O_3P\text{-}(CH_2)_3\text{-}PO_3\}\cdot 2H_2O$ by using (a) an isolated spin dimer model and (b) An alternating Heisenberg AFM 1D chain model, respectively. The dotted lines indicate the observed magnetic susceptibility (ref. 13) and the red lines indicate the fitting results.

atoms of a SSE path is strongly increased when the basal planes are coplanar.[7b,20] Therefore, we can expect that the spin exchange interaction of the SSE path J_2 is stronger than those of the SSE paths J_3 and J_4. It is difficult, however, to compare the relative strengths between SE and SSE paths without proper electronic structure calculations. Relative values of $(\Delta e)^2$ for the spin dimes are shown in Table 2. Our calculations were carried out using the atomic orbital parameters collected in Table 3. There are two strongly interacting spin exchange paths J_1 and J_2. The J_1 is SE interaction and the J_2 is SSE interaction. The spin exchange interactions of the SSE paths J_3 and J_4 are negligibly weak. The strongest spin exchange interaction occurs the SSE path J_2 and the second strongest spin exchange interaction occurs through the SE path J_1. The paths J_1 and J_2 alternate along the c-direction. Therefore, two strongly interacting spin exchange paths J_1 and J_2 lead an alternating chain along the c-direction. Since both spin exchange interactions J_1 and J_2 are AFM and responsible for the magnetic properties of $(VO)_2(H_2O)\{O_3P\text{-}(CH_2)_3\text{-}PO_3\}\cdot 2H_2O$, we can predict that a proper spin-lattice model for $(VO)_2(H_2O)\{O_3P\text{-}(CH_2)_3\text{-}PO_3\}\cdot H_2O$ is an alternating spin-1/2 AFM chain along the c-direction rather than the isolated spin dimer. To confirm whether the observed magnetic susceptibility curve can be reproduced by the alternating AFM chain model, we fitted the magnetic susceptibility curve by using the alternating Heisenberg AFM chain model with two J_1 and J_2 parameters. The observed magnetic susceptibility curve is perfectly well fitted when we introduce spin exchange interactions between the adjacent spin dimers. It means that the spin exchange

interaction between the spin dimers cannot be ignored and the isolated spin dimer model is not suitable spin-lattice model for $(VO)_2(H_2O)\{O_3P\text{-}(CH_2)_3\text{-}PO_3\}\cdot H_2O$. This result agrees with the suggestion of Riou *et al*.[13] that the spin exchange interaction between adjacent spin dimers which is not taken into account in the Bleaney-Bowers equation cannot be ignored. The best fit for the magnetic susceptibility curve is observed by using the alternating Heisenberg AFM chain model with $J_2 = -87$ K and $J_2/J_1 = 0.15$. The numerically analyzed magnetic susceptibility curves are shown in Figure 4.

To know how the values of diffuseness of the O 2p orbital affects the relative strengths of spin exchange interactions, we change ζ_2 with $(1\text{-}x)\zeta_2$ and calculate the $(\Delta e)^2$ values for three values of x, that is 0.00, 0.05 and 0.10. As summarized in Table 2, the picture of spin exchange interactions does not depend on the variation of the diffuseness of the O 2p orbital, i.e., the SSE path J_2 and the SE path J_1 are the strongest spin exchange paths.

Concluding Remarks

Strong spin exchange interactions in $(VO)_2(H_2O)\{O_3P\text{-}(CH_2)_3\text{-}PO_3\}\cdot 2H_2O$ take place through the spin exchange path J_1 and J_2. The relative strength of the SSE path J_2 is stronger than the SE path J_1. These two spin exchange paths alternate along the c-direction, so they lead an alternating AFM chain consisted of J_1-J_2 spin exchange interactions. The better fitting result for the observed magnetic susceptibility curve is obtained when we use the alternating Heisenberg AFM chain model rather than the isolated spin dimer model. Therefore, we can predict that the precise spin-lattice model, to describe the magnetic properties of $(VO)_2(H_2O)\{O_3P\text{-}(CH_2)_3\text{-}PO_3\}\cdot 2H_2O$, is the alternating Heisenberg AFM chain.

Acknowledgments. This research was supported by the Kyung Hee University Research Fund in 2008. (KHU-20080534) HJK thanks Dr. Dai for the numerical analysis of magnetic susceptibility.

References

1. Koo, H.-J.; Whangbo, M.-H. *Inorg. Chem.* **2000**, *39*, 3599.
2. For reviews see: (a) Whangbo, M.-H.; Koo, H.-J.; Dai, D. *J. Solid State Chem.* **2003**, *176*, 417. (b) Whangbo, M.-H.; Dai, D.; Koo, H.-J. *Solid State Sci.* **2005**, *7*, 827.
3. Koo, H.-J.; Dai, D.; Whangbo, M.-H. *Inorg. Chem.* **2005**, *44*, 4359.
4. Koo, H.-J.; Whangbo, M.-H. *Inorg. Chem.* **2006**, *45*, 4440.
5. Koo, H.-J.; Whangbo, M.-H. *Inorg. Chem.* **2008**, *47*, 128.
6. Koo, H.-J.; Whangbo, M.-H. *Inorg. Chem.* **2008**, *47*, 4779.
7. (a) Koo, H.-J.; Whangbo, M.-H. *Inorg. Chem.* **2001**, *40*, 2169. (b) Koo, H.-J.; Whangbo, M.-H.; VerNooy, P. D.; Torardi, C. C.; Marshall, W. J. *Inorg. Chem.* **2002**, *41*, 4664. (c) Whangbo, M.-H.; Koo, H.-J.; Dai, D.; Jung, D. *Inorg. Chem.* **2003**, *42*, 3898. (d) Koo, H.-J.; Whangbo, M.-H.; Lee, K.-S. *Inorg. Chem.* **2003**, *42*, 5932. (e) Dai, D.; Koo, H.-J.; Whangbo, M.-H. *Inorg. Chem.* **2004**, *43*, 4026. (f) Koo, H.-J.; Dai, D.; Whangbo, M.-H. *Inorg. Chem.* **2005**, *44*, 4359. (g) Bae, H. W.; Koo, H.-J. *Bull. Korean Chem. Soc.* **2008**, *29*, 122.
8. Johnston, D. C.; Johnson, J. W.; Goshorn, D. P.; Jacobson, A. J. *Phys. Rev. B* **1987**, *35*, 219.
9. Barnes, T.; Riera, J. *Phys. Rev. B* **1994**, *50*, 6817.
10. Eccleston, R. S.; Barnes, T.; Brody, J.; Johnson, J. W. *Phys. Rev. Lett.* **1994**, *73*, 2626.
11. Garret, A. W.; Nagler, S. E.; Tennant, D. A.; Sales, B. C.; Barnes, T. *Phys. Rev. Lett.* **1997**, *79*, 745.
12. Kikuchi, J.; Motoya, K.; Yamauchi, T.; Ueda, Y. *Phys. Rev. B* **1999**, *60*, 6731.
13. Riou, D.; Serre, C.; Provost, J.; Ferey, G. *J. Solid State Chem.* **2000**, *155*, 238.
14. Bleaney, B.; Bowers, K. D. *Proc. Roy. Soc. (London) Ser. A* **1952**, *214*, 451.
15. (a) Johnson, J. W.; Johnston, D. C.; Jacobson, A. J.; Brody, J. F. *J. Am. Chem. Soc.* **1984**, *106*, 8123. (b) Johnston, D. C.; Johnson, J. W. *J. Chem. Soc. Chem. Commun.* **1985**, *23*, 1720.
16. Hay, P. J.; Thibeault, J. C.; Hoffmann, R. *J. Am. Chem. Soc.* **1975**, *97*, 4884.
17. Hoffmann, R. *J. Chem. Phys.* **1963**, *39*, 1397.
18. Our calculations were carried out by employing the SAMOA (Structure and Molecular Orbital Analyzer) program package (Dai, D.; Ren, J.; Liang, W.; Whangbo, M.-H. http://chvamw.chem.ncsu.edu/, 2002).
19. Clementi, E.; Roetti, C. *At. Data Nucl. Data Tables* **1974**, *14*, 177.
20. Koo, H.-J.; Whangbo, M.-H. *Solid State Sci.* **2010**, *12*, 685.